



## ACTIVE CONTROL OF FLOW BEHIND A BACKWARD FACING STEP BY USING A PERIODIC PERTURBATION

Zouhaier Mehrez<sup>1</sup>, Mourad Bouterra<sup>1</sup>, Afif El Cafsi<sup>1</sup>, Ali Belghith<sup>1</sup> and Patrick Le Quéré<sup>2</sup>

<sup>1</sup>Faculté des Sciences de Tunis-Campus Universitaire, 1060 Tunis Tunisia

<sup>2</sup>LIMSI-CNRS Bat 508 - B.P. 133 - 91 403, Orsay Cedex, France

E-Mail: [zouhaier.mehrez@yahoo.fr](mailto:zouhaier.mehrez@yahoo.fr)

### ABSTRACT

In this paper the active control of the turbulent separated and reattaching flow over a backward facing step is studied numerically by the Large Eddy Simulation (LES) method. The objective of the control consists to modify the separation phenomenon of the fluid in the edge of the step by application a periodic perturbation. The perturbation is realized by zero-net alternative suction and blowing of the fluid in the step edge into separated shear layer. The found results showed the reduction of the reattachment length and the enhancement of the shedding vortical frequency by the applied periodic perturbation. Also, the existence of an optimum frequency,  $St_p = 0.25$ , in term of promotion of reattachment and the increase of shedding vortical frequency. At this perturbation frequency an important modification of the dynamic of the flow is observed. The modifications observed at the optimum frequency are noticeable as the perturbation amplitude increases.

**Keywords:** backward-facing step, large eddy simulation, vortical shedding frequency, periodic perturbation.

### 1. INTRODUCTION

The performance of fluid machinery is influenced by the occurrence of the flow separation and reattachment phenomena. Separated flows show positive and negative effects depending on the application. A desired recirculation region as a result of a separation is needed in combustion chambers to keep the fuel mixture in the reaction zone for a complete combustion. By influencing a recirculation zone, the residence time behaviour in general mixing problem is altered. In contrast to that, negative consequences could be a loss in efficiency and noise production in turbo-machines or process plant such a diffusors.

Thus, the suppression or desired control of separation phenomena has been addressed in the mechanics community for many decades. There has been much research interest on the periodically perturbed turbulent separated flow. Singurdson [8], Chun and Sung [3] are interested to the active control of the reattachment process, in which the enhancement of momentum transport across the separated shear layer plays a major role. Several authors are interested to the excitation of the instability and vortex formation inherent to the separated shear layer (Bhattacharjee *et al.*, [1]; Kiya *et al.*, [5]; Chun and Sung, [4]; Yoshioka *et al.*, [10]).

In this paper, by using a numerical simulation LES, we interest to the influence of the active control on the dynamic, size of recirculation zone and the shedding vortical phenomenon in the separated and reattaching flow over a backward facing step.

### 2. NUMERICAL SIMULATION

#### 2.1 Basic equations

The conservation equations describing the flow are the time-dependent, 2D Navier-Stokes equations and the conservation equation for a constant-property incompressible fluid. For the flows considered here, the

basic governing equations are written in the filtered dimensionless form as:

$$\begin{aligned} \square \frac{\partial \bar{u}_i}{\partial x_i} &= 0 \\ \square \frac{\partial \bar{u}_i}{\partial t} + \frac{\partial (\bar{u}_i \bar{u}_j)}{\partial x_j} &= -\frac{\partial \pi}{\partial x_i} + \frac{\partial}{\partial x_j} \left( \frac{1}{Re} \frac{\partial \bar{u}_i}{\partial x_j} \right) - \frac{\partial (\tau_{ij})}{\partial x_j} \end{aligned}$$

The bar in the LES equations denotes a filtered or large-scale flow quantity. The governing dimensionless parameter appearing in the above equations is the Reynolds number ( $Re = \frac{U_0 h}{\nu}$ ). When  $U_0$  denote the reference values of streamwise mean velocity and  $\nu$  is the kinematics viscosity. The modified pressure is given by:  $\pi = \bar{p} + \frac{1}{3} \tau_{kk}$ .

The Subgrid scale Reynolds stress is estimated by means of the eddy viscosity model:  $\tau_{ij} = 2\nu_t \bar{S}_{ij}$ . The turbulent viscosity is given by

$$\nu_t = c_m |\bar{S}|^\alpha (q_c^2)^{(1-\alpha)/2} \Delta^{(1+\alpha)}. \text{ When considering}$$

homogeneous isotropic turbulence, and  $\alpha = 0.5$  (the value retained throughout this work), the theoretical value of the parameter  $c_m$  is found equal to 0.04 on the basis of an equilibrium assumption between the dissipation and energy-transfer rates. The characteristic length scale is usually chosen to be  $\Delta = \sqrt{\Delta x \Delta y}$ , where  $\Delta x$  and  $\Delta y$  are mesh sizes in the x- and y-directions respectively. The second invariant of the shear stress tensor is given

$$\text{by } |\bar{S}| = (\bar{S}_{ij} \bar{S}_{ij})^{1/2}, \text{ where } \bar{S}_{ij} = \frac{1}{2} \left( \frac{\partial \bar{u}_i}{\partial x_j} + \frac{\partial \bar{u}_j}{\partial x_i} \right)$$

is the strain rate tensor of the filtered flow field, and the kinetic



energy  $q_c^2$  is obtained by the scale similarity assumption, and by means of a double-filtering technique:

$$q_c^2 = \frac{1}{2}(\bar{u}_i - \hat{u}_i)^2, \text{ where } (\hat{\cdot}) \text{ represents a filter with a cut-off length of } 2\Delta. \text{ The explicit filter used here is a local weighted-average } \hat{u}_i = \frac{1}{4}\bar{u}_{i-1} + \frac{1}{2}\bar{u}_i + \frac{1}{4}\bar{u}_{i+1}.$$

The mixed Subgrid scale model is a self-adapted model because the eddy viscosity vanishes automatically at the wall and in the regions of the flow where all the structures are well resolved.

## 2.2 Numerical resolution

A finite volume method is adapted to the standard staggered grid in which pressure and velocity components are stored at different points. On the other hand, we have used the projection (fractional step) method (Chorin [2] and Temam [9]) for decoupling pressure from velocity. The space discretization uses a second order upwind finite difference method by means of a QUICK scheme, proposed by Leonard [6] for the convective terms and a centered scheme for the diffusive ones.

## 3. COMPUTATIONAL DOMAIN AND BOUNDARY CONDITIONS

Two-dimensional flow behind a backward-facing step subjected to a sinusoidal perturbation is simulated. The computational domain and the coordinates system are represented in Figure-1. Channel expansion ratio is fixed at  $H/h = 3$  in all the study. The Reynolds number is fixed at 33000. To control the flow, Chun and Sung [4], Yoshioka *et al.* [10], experimentally introduced a periodic forcing by pulsating jet (blowing and suction of the fluid) at the edge of the step. In this work, we have simulated such a disturbance by introducing a local velocity  $u = A\sin(2\pi ft)$  (Figure-1.), where  $A$  and  $f$  are respectively the amplitude and the frequency disturbance. At the channel inlet, a fully developed parabolic profile for the velocity is deployed. At the exit, convective boundary

conditions for all variables ( $\frac{\partial u}{\partial x} = \frac{\partial v}{\partial x} = 0$ ) are set. No-

slip conditions are prescribed at the body surfaces ( $u = v = 0$ ). At the upper boundaries, symmetry conditions simulating a frictionless wall are used ( $\frac{\partial u}{\partial y} = v = 0$ ).

The time step is  $\Delta t = 4 \cdot 10^{-3}$ , close to the stability limit. Several trial calculations were repeated to monitor the sensitivity of the results to grid resolution. The grid convergence was checked, the outcome of these tests (104x66 uniform fine grid) was found to be satisfactory. The simulation of the flow over a sufficiently large dimensionless time interval ( $tU_0/H = 400$ ) allowed us to be sure that the asymptotic regime is reached.

## 4. RESULTS AND DISCUSSIONS

### 4.1 Flow without perturbation

The normal velocity  $v$  contours are presented in the Figure-2. The negative contours are plotted using dashed lines and the positive contours using solid lines. The negative  $v$ -contours, noticed in the outer (zone of shear layer) and downstream regions of the reattachment all around the recirculation bubble, indicate that most of the flow is directed downward. This must be essentially due to the turbulent activity of the external big eddies towards the wall. In the reattachment region (downstream of recirculation), we can observe also high values in the normal gradient of the  $v$ -velocity component. Also, we can again notice the two counter-rotating bubbles in the recirculation zone, downstream of the step.

The value of the time-mean reattachment length (indicate in the Figure-2 by a triangle) in the experiment of Chun and Sung [4] is  $X_{r0} = 7.4h$ , our simulations give a value of  $X_{r0} = 7.2h$ . The agreement between the computation and the experiment is rather good.

### 4.2 Effects of the perturbation on the flow

In this section the amplitude of the perturbation is fixed at  $A = 0.3U_0$ . The perturbation frequency is presented by the dimensionless Strouhal number of perturbation  $St_p = f_p h / U_0$ . Where  $h$  is the height of the step,  $f_p$  the perturbation frequency and  $U_0$  the streamwise velocity in the inlet.

#### 4.2.1 Effect on the reattachment length

The perturbation frequency varied in the range  $0 \leq St_p \leq 2$ . The normalized reattachment length,  $X_r/X_{r0}$  is plotted in Figure-3 as a function of the Strouhal number  $St_p$ . The experimental data of Chun and Sung [4] and the numerical works using the  $k-\epsilon-f_\mu$  model (Rhee *et al.*, [7]) are also included for comparison.  $X_r$  varies by variation of the perturbation frequency. The minimum observed at the optimum frequency,  $St_p = 0.25$ , in terms of the reduced reattachment length. The agreement between the computation and the experiment is satisfactory, in particular, the optimum frequency ( $St_p = 0.25$ ) in the experiment is clearly reproduced by the present simulation.

#### 4.2.2 Effect on the profiles of velocity

The profiles of mean velocities are represented in the Figure-4 for four different sections of the flow. These profiles are carried out for four frequencies of perturbation:  $St_p = 0$  (non-perturbed flow),  $St_p = 0.05$  (lower than the optimum frequency),  $St_p = 0.25$  (optimum frequency) and  $St_p = 1$  (higher than the optimum frequency). We can note the presence of negative longitudinal velocity  $u$ , in the zone of recirculation ( $x/X_r \leq 1$ ); in all cases (see Figure-4.a). These velocities become more significant by applied perturbation. The reverse flow in the recirculation zone is more significant at the optimum frequency. This result shows that the rotating velocity enhances in the recirculation zone by applied



perturbation. Downstream of the reattachment zone ( $x/X_r \geq 1$ ) the acceleration of the fluid is observed with two frequencies ranges (the lower and the higher frequencies than the optimum frequency) in the central region of the shear layer (around  $y/H = 0.3$ ). On the other hand, at the optimum frequency  $St_p = 0.25$ , the acceleration of fluid is observed in the external region of the boundary layer which develops downstream of reattachment ( $x/X_r \geq 1$ ). We can conclude that the perturbation accelerates the flow in the shear layer, but this depends on the imposed perturbation frequency. In the Figure-4.b the profiles of mean normal  $v$ -velocity are represented in the different sections. These profiles confirm the result illustrates the acceleration of the fluid in the different zones of the perturbed flow. We can note also that the motion downward of fluid around the recirculation zone enhances by perturbation. This effect becomes noticeable at the optimum perturbation frequency  $St_p = 0.25$ .

#### 4.2.3 Effect on the vortical shedding frequency

The vortical shedding frequency in the reattachment zone is presented by the dimensionless Strouhal number of shedding  $St_s = f_s h / U_o$ . Where  $f_s$  is the vortical shedding frequency.

The temporal evolution of longitudinal  $u$ -velocity, in the reattachment zone, and its frequencies spectra are represented in Figure-5 for different Strouhal numbers of perturbation. In all the studied cases, the velocity oscillates, while changing of sign, around a mean value (see Figure-5.a). This indicates that the reattachment is governing by a eddies vortical activity. The augmentation of the oscillating amplitude of the velocity, in the perturbed flow case, shows that the vortical activity becomes more significant. The Figure-5.b shows the spectrum of longitudinal velocity obtained by Fourier transformation at the same locations. In the all considered cases, we note the presence of a dominant peak which presents the fundamental frequency correspondent to shedding vortical frequency. This frequency increases by introduction the periodic perturbation in the flow. The amplitude of dominant peak becomes more significant in the perturbed flow. This confirms that the intensity of vortexes becomes more important by applied perturbation.

The Figure-6 shows the variations of the Strouhal number of vortical shedding  $St_s$  as a function of Strouhal number of perturbation  $St_p$  for various normalized perturbation amplitude  $A/U_o$ . For the all perturbation amplitude the vortical shedding frequency varies by variation of the perturbation frequency. The peak is obtained, in the all cases, at the optimum perturbation frequency  $St_p = 0.25$ . This value of the perturbation

frequency is also optimum in term of increase of vortical shedding frequency.

In Figure-7 the temporal evolution of longitudinal velocity  $u$  and their spectrum are plotted for different perturbation amplitude at the optimum perturbation frequency,  $St_p = 0.25$ . By augmentation of perturbation amplitude, the amplitude of oscillation increases (see Figure-7.a.). These oscillations become more organized of the point of view amplitude which takes a constant value and also of the point of view period. The spectra (see Figure-7.b) show that by increasing the perturbation amplitude, the amplitude of the dominant peak (represents the shedding vortical frequency) increases and its harmonics become clearer. This shows that the coherent structures become more intense and the flow becomes more organized.

The found results show that the shedding process is modified by the applied perturbation. Indeed the shear layer above the recirculation zone is the seat of formation of coherent vortical structures. These vortexes that are convecting downstream are responsible for the entrainment out of the recirculation zone. By stimulating their growth through applying a perturbation, the increased shear layer growth rate leads to a significant reduction of the size of the recirculation zone and, hence, a reduction in residence time, consequently the shedding vortical frequency increases. These effects are noticeable by increasing the perturbation at the optimum frequency,  $St_p = 0.25$ .

## 5. CONCLUSIONS

The numerical study of the periodically perturbed separated and reattaching flow over a backward facing step is investigated by the Large Eddy Simulation methodology. The model capability is validated by comparing the numerical simulation with the experiment. The reattachment length varies with the applied perturbation frequency and the maximum shortened attains at the optimum perturbation frequency,  $St_p = 0.25$ . Corresponding to this promotion of reattachment, the velocity of rotation of the fluid in the recirculation zone enhances and the vortical activity at the shear layer becomes more significant. This reduces the residence time of the vortexes and enhances the shedding vortical frequency. The flow becomes more organized by increasing the perturbation amplitude at the optimum perturbation frequency. The found results show the possibility of controlling the instabilities existing in the separated and reattaching flow by application of a periodic perturbation.

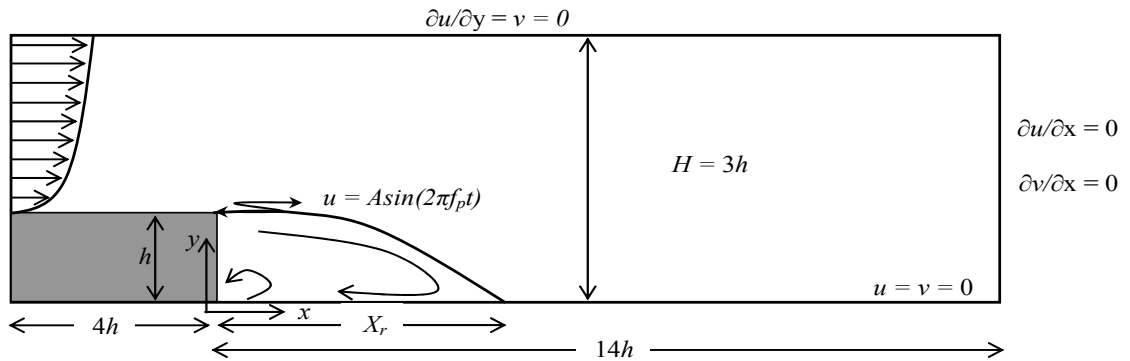


Figure-1. Geometric configuration of computational domain.

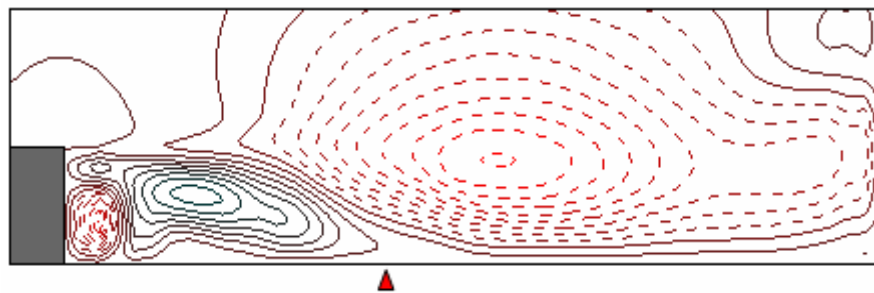


Figure-2. Contours of the normal velocity component v.

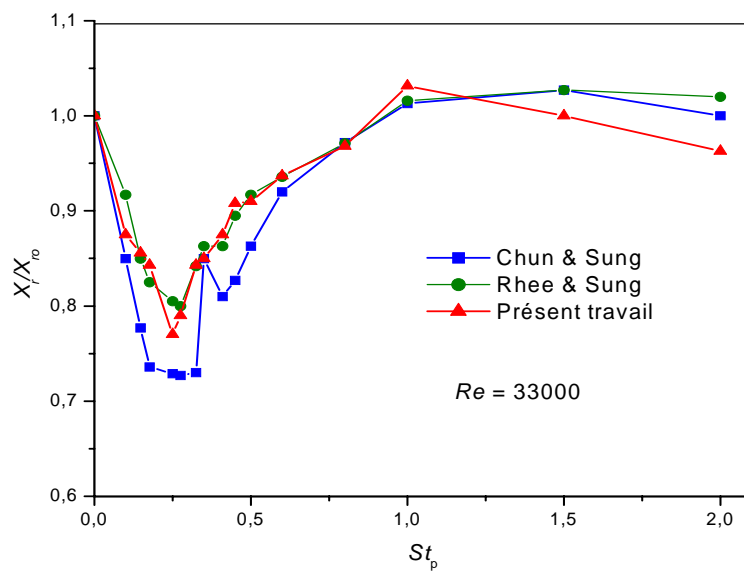
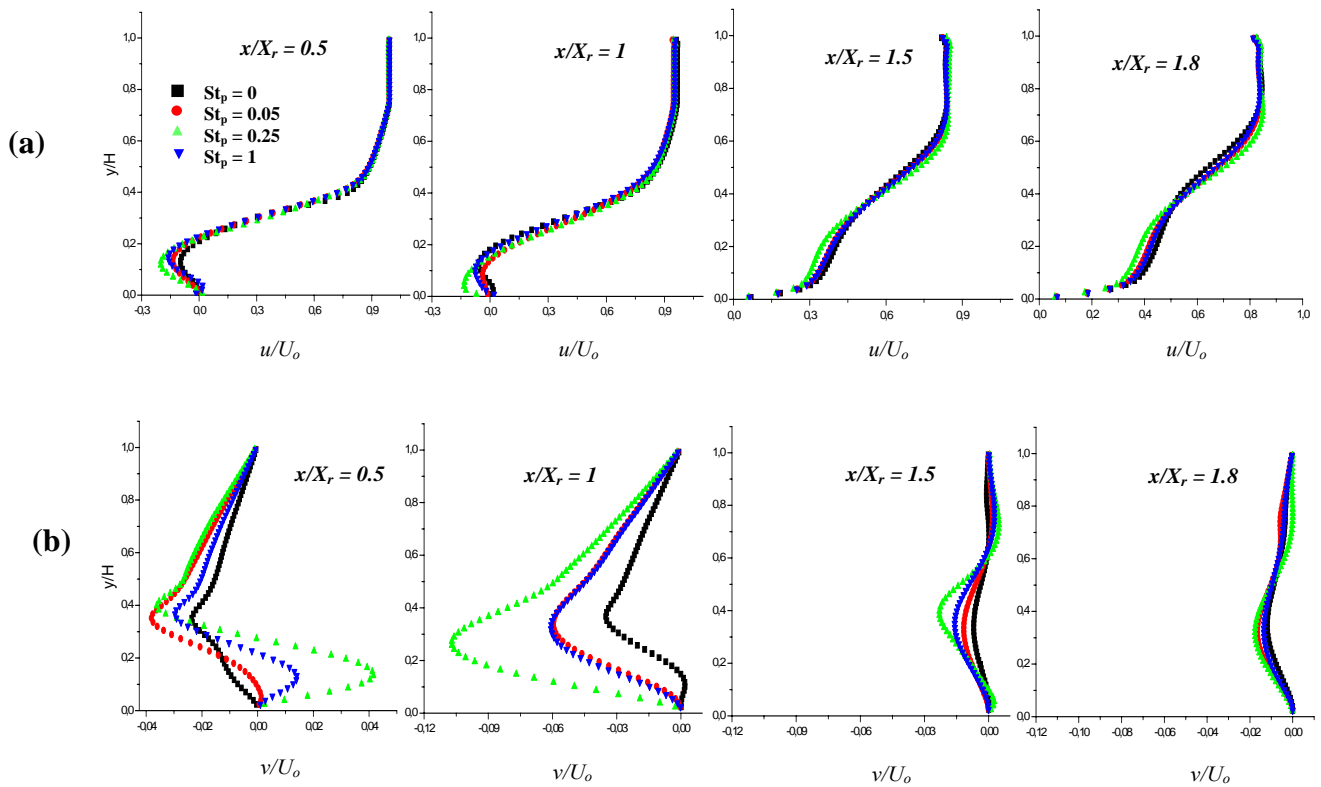
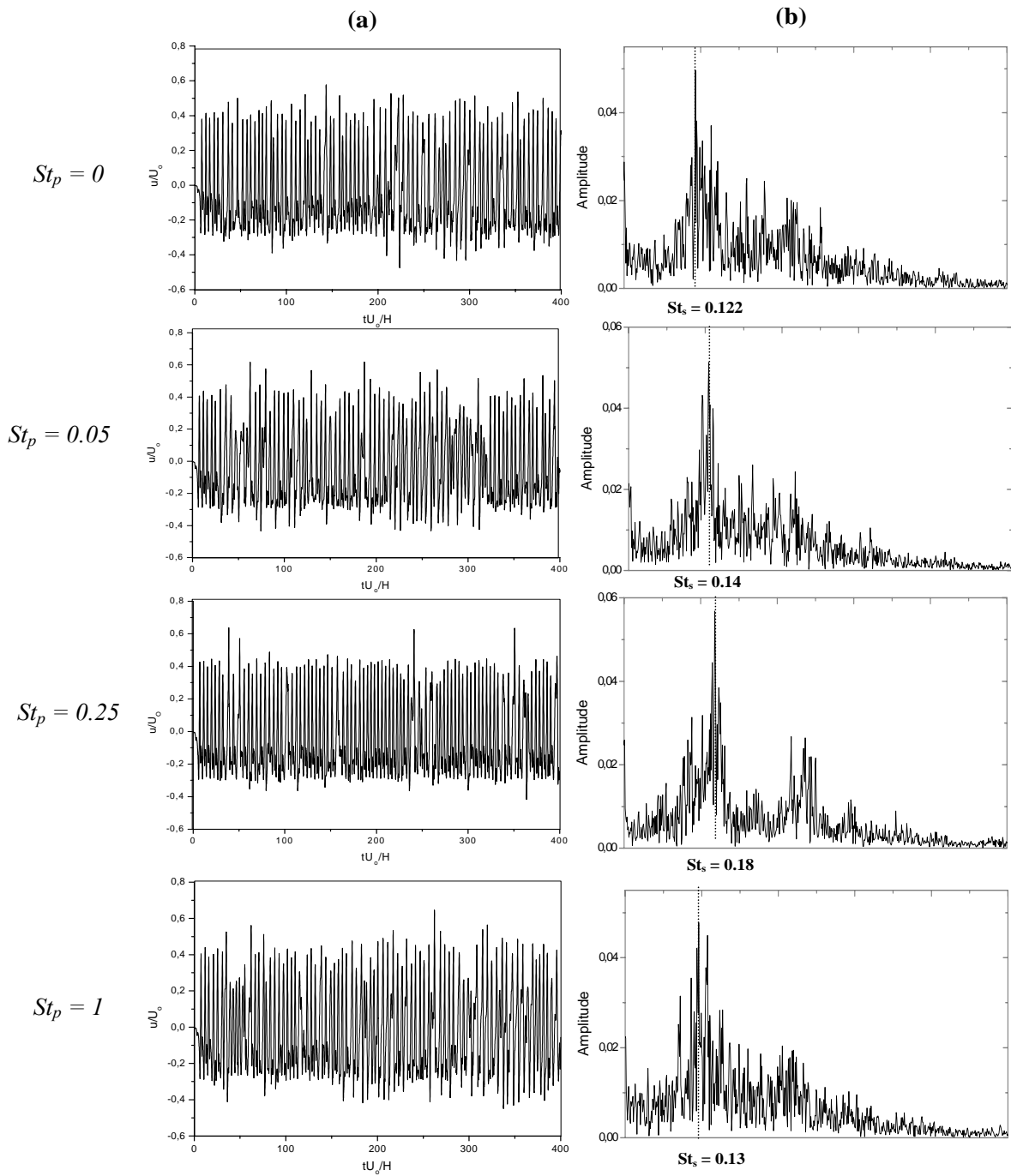


Figure-3. Normalized reattachment length  $X_r/X_{r0}$  against  $St_p$ .



**Figure-4.** Mean velocity profiles at various streamwise locations: (a) longitudinal velocity component  $u$ ; (b) normal velocity component  $v$ .



**Figure-5.** a) Temporal evolution of the longitudinal velocity  $u$  in the reattachment region; b) spectrum of the longitudinal velocity  $u$  in the reattachment region for various  $St_p$ .

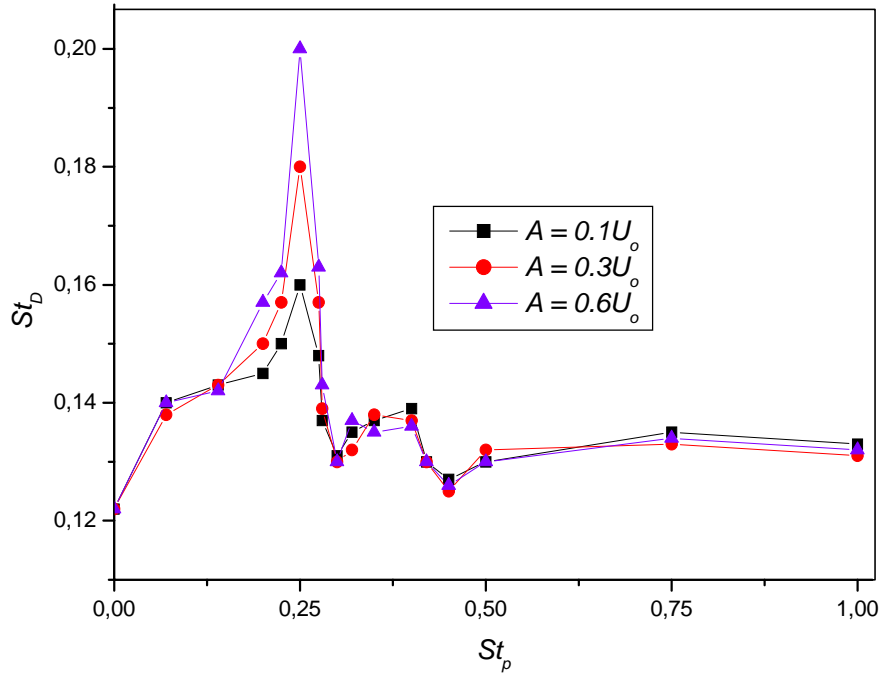


**Figure-6.** Strouhal number of vortical shedding frequency  $St_s$  against strouhal number of perturbation  $St_p$  for various perturbation amplitude.

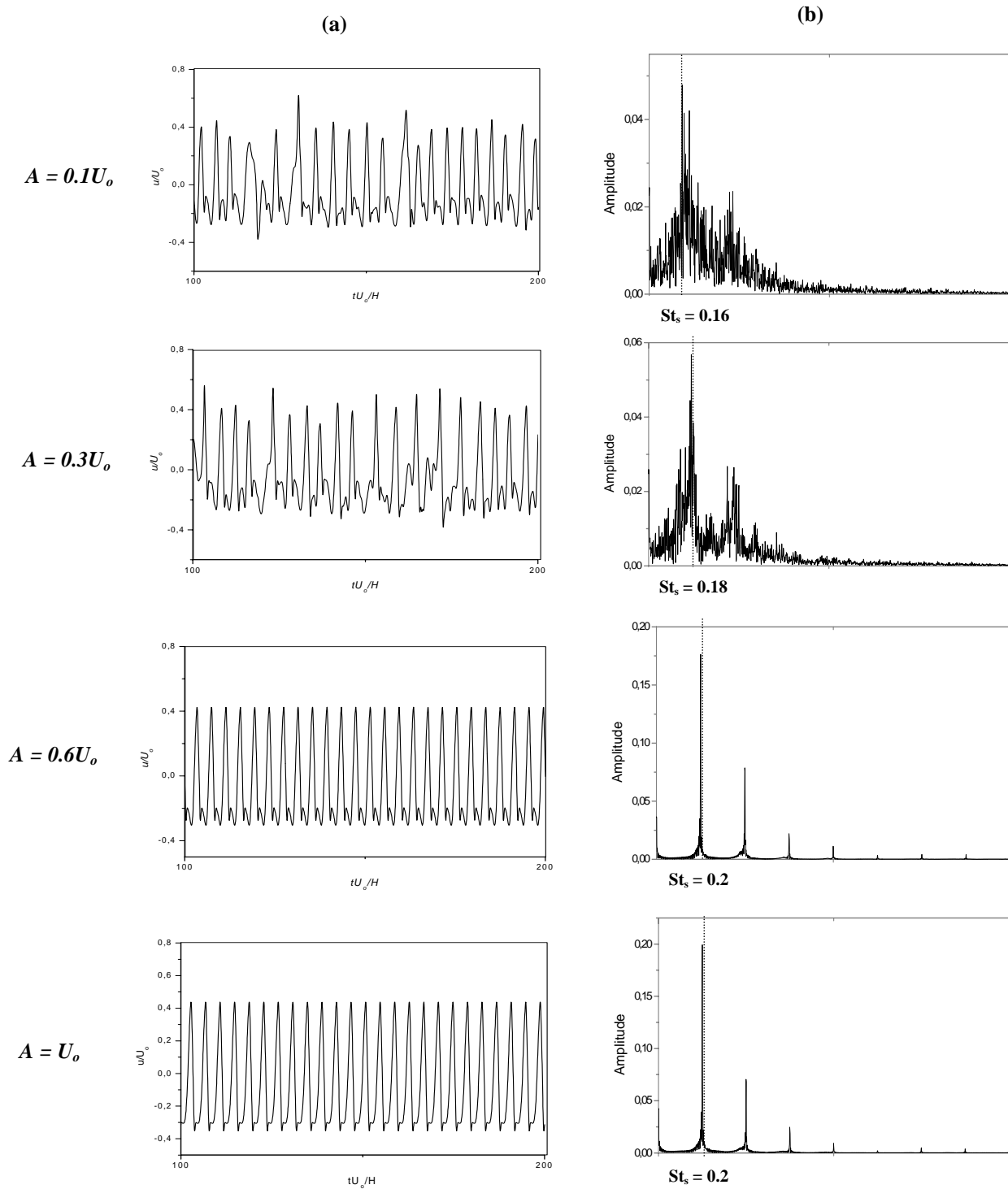


**Figure-7.** a) Temporal evolution of the longitudinal velocity  $u$  in the reattachment region; b) spectrum of the longitudinal velocity  $u$  in the reattachment region for various perturbation amplitude.



**REFERENCES**

- [1] Bhattacharjee S., B. Scheelke and T.R. Troutt. 1986. Modification of vortex interaction in a reattaching separated flow. *AIAA*. 24: 623-629.
- [2] Chorin A. 1968. Numerical simulation of the Navier-Stokes equations. *J. Math. Comput.* 22: 745-762.
- [3] Chun K.B., H.J. Sung. 1996. Control of turbulent separated flow over a backward-facing Step by local forcing. *Exp. Fluids*. 21: 133-142.
- [4] Chun K.B., H.J. Sung. 1998. Visualization of a locally-forced separated flow over a backward-facing Step. *Exp. Fluids*. 25: 417-426.
- [5] Kiya M., M. Shimizu O. Mochizuki. 1997. Sinusoidal forcing of a turbulent separation bubble. *J. of Fluid Mechanics*. 330: 349-374.
- [6] Leonard. B.P. 1988. Simple high accuracy resolution program for convection modelling of discontinuities. *Int. J. for Num. Methods in fluids*. 8: 1291-1318.
- [7] Rhee G.H., H.J. Sung. 2000. Turbulent numerical prediction of locally forced separated and reattaching flow. *Fluid Dynamics Research*. 26: 421-436.
- [8] Sigurdson L.W. 1995. The structure and control of a turbulent reattaching flow. *J. of Fluid Mechanics*. 298: 139-165.
- [9] Temam R. 1968. Une méthode d'approximation de la solution des équations de Navier-Stokes, *Bull. Soc. Math. France*. 98: 115-152.
- [10] Yoshioka S., S. Obi., S. Masuda. 2001. Organized vortex motion in periodically perturbed turbulent flow over a backward-facing step. *Int. J. Heat Fluid Flow*. 22: 301-307.